

## N-polar III-nitride quantum well light-emitting diodes with polarization-induced doping

Jai Verma, John Simon, Vladimir Protasenko, Thomas Kosel, Huili Grace Xing, and Debdeep Jena<sup>a)</sup>

Department of Electrical Engineering, University of Notre Dame, Indiana 46556, USA

(Received 11 June 2011; accepted 4 October 2011; published online 25 October 2011)

Nitrogen-polar III-nitride heterostructures present unexplored advantages over Ga(metal)-polar crystals for optoelectronic devices. This work reports N-polar III-nitride quantum-well ultraviolet light-emitting diodes grown by plasma-assisted molecular beam epitaxy that integrate polarization-induced p-type doping by compositional grading from GaN to AlGaIn along N-face. The graded AlGaIn layer simultaneously acts as an electron blocking layer while facilitating smooth injection of holes into the active region, while the built-in electric field in the barriers improves carrier injection into quantum wells. The enhanced doping, carrier injection, and light extraction indicate that N-polar structures have the potential to exceed the performance of metal-polar ultraviolet light-emitting diodes.

© 2011 American Institute of Physics. [doi:10.1063/1.3656707]

III-nitrides are direct gap semiconductors that span a large range of energies ranging from 0.7 eV (InN) through 3.4 eV (GaN) to 6.2 eV (AlN). This makes them uniquely suited for visible<sup>1</sup> and ultraviolet light-emitting diodes (UV LEDs).<sup>2</sup> The built-in polarization-induced electric field in wurtzite III-nitrides<sup>3</sup> has led to their application in high electron mobility transistors (HEMTs) and Zener tunnel diodes.<sup>4-6</sup> But polarization is often viewed as deleterious for heterostructure quantum-well (QW) light emitters due to the reduction of the oscillator strength of optical transitions by the quantum-confined Stark effect.<sup>7</sup> As growth of GaN heterostructures along the N-polar crystal orientation matures, it is timely to investigate its potential advantages in electronic and optoelectronic devices. It has been found that N-polar structures are advantageous for HEMTs,<sup>8,9</sup> Zener tunnel diodes,<sup>10</sup> and photovoltaic devices.<sup>11</sup> Recently, N-polar 540 nm green LED has been demonstrated.<sup>12</sup> In this work, we discuss the potential benefits of N-polar LEDs and then demonstrate N-polar QW LED with integrated polarization-induced p-type doping.

The overall conversion efficiency of LEDs is given by the product  $\eta_{tot} = \eta_{inj} \times \eta_{rad} \times \eta_{extr}$ , where the three efficiencies are the injection, radiative, and extraction efficiency, respectively. Wide-bandgap III-nitrides suffer from poor p-type conductivity because of the large activation energy ( $E_A$ ) for Mg acceptor dopants (Refs. 13 and 14). Since  $E_A \gg kT$  ( $k$ : Boltzmann constant,  $T$ : temperature) at room temperature, the low-level of thermal ionization results in poor hole concentration and consequently low  $\eta_{inj}$ . Recently, polarization engineering and asymmetric QW have been used to improve the electron and hole injection into the active region of metal-polar 273 nm UV LED.<sup>15</sup> Besides, polarization-induced p-type doping by compositionally grading GaN to AlGaIn along N-face has been demonstrated to increase  $\eta_{inj}$  by improving conductivity in III-nitride UV LEDs.<sup>16</sup> Moreover the higher bandgap graded p-type layer would stop the re-absorption of emitted light by itself,

resulting in higher  $\eta_{extr}$ . Traditional electron blocking layers (EBL) are sharp AlGaIn/GaN heterojunctions, as shown in Fig. 1(a) in which the unavoidable valence band offset also blocks hole injection and decreases  $\eta_{inj}$ . In N-polar structures the polarization-induced p-doped cap layer acts simultaneously as an electron blocking layer while removing any energy barriers from the path of holes as shown in the energy band diagrams (simulated using SimuAPSYS) in Fig. 1(b). This feature has been demonstrated by Wang *et al.*<sup>17</sup> as a solution to the efficiency droop problem in InGaIn/GaN light

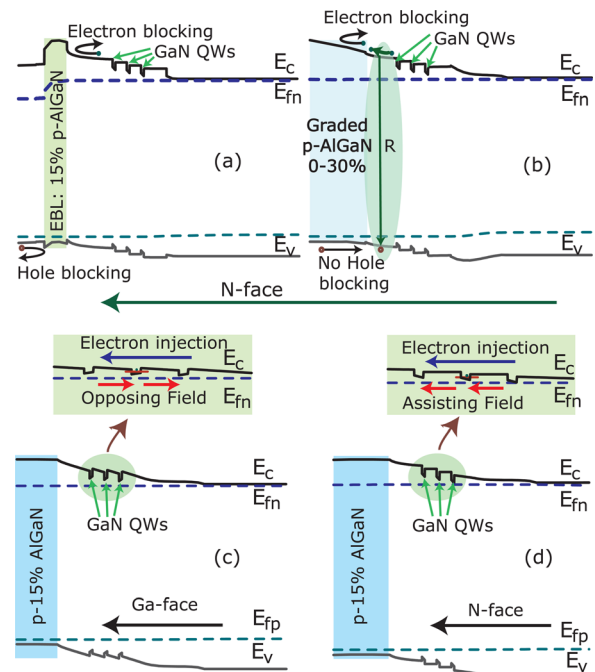


FIG. 1. (Color online) Simulated energy band diagrams showing the advantages of N-polar light-emitting nitride heterostructures with GaN/Al<sub>0.15</sub>Ga<sub>0.85</sub>N MQW. (a) N-polar QW LED structure with EBL and (b) polarization-induced p-type doping. (c) Ga-face quantum well LED structure: polarization fields in the AlGaIn barrier layers oppose injection of electrons (and holes) into the QWs. (d) N-face quantum well LED structure showing the polarization fields assist in carrier injection into the QWs.

<sup>a)</sup>Electronic mail: djena@nd.edu.

emitting diodes grown along Ga-face GaN substrate with the p-type layer at the bottom (hole injection along [0001]).

The advantages of N-polar heterostructures are not restricted to the ease of integration of polarization-induced doping alone. For hole injection along the [000 $\bar{1}$ ] direction in III-nitride QW LED structures, polarization-induced electric field in the barrier region *opposes* [Fig. 1(c)] the injection of electrons and holes into the QWs. But when the hole injection is along the [0001] direction, the electric field *assists* (Fig. 1(d)) carrier injection into the QWs, thus increasing  $\eta_{inj}$ . Figs. 1(c) and 1(d) show simulated energy band diagrams which illustrate this phenomenon for GaN QWs incorporated between Al<sub>0.15</sub>Ga<sub>0.85</sub>N barriers on Ga-face and N-face GaN substrate, respectively. Moreover, N-polar III-nitrides can be grown at higher temperatures compared to metal-polar leading to better crystal quality.<sup>18</sup> This reduces the non-radiative recombination centers in the crystal and increases  $\eta_{rad}$ . Besides,  $\eta_{extr}$  has been shown to increase for III-nitride based LEDs by surface roughening through photoelectrochemical wet etching of N-face<sup>19</sup> which is the far more chemically active crystal face in III-nitride semiconductors.<sup>20</sup>

We now report the realization of QW UV-LEDs on N-face GaN integrated with polarization-induced p-type doping. Polarization-doped ( $\pi$ -doped) AlGaIn-GaN p-n heterojunctions were grown without (device A) and with (device B) GaN QWs with the growth performed along N-face using plasma assisted molecular beam epitaxy (PAMBE) on commercially available n-type free-standing N-face GaN substrates. The growth was performed under metal-rich conditions, and a constant nitrogen RF power (275 W) was maintained. The Al flux from an effusion cell is exponentially dependent on the temperature of the effusion cell  $F_{Al} \exp(-E_{Al}/k_b T_{Al})$ , where  $E_{Al}$  is the activation energy,  $T_{Al}$  is the Al cell temperature, and  $k_b$  is the Boltzmann constant. To achieve linear compositional grading,  $T_{Al}$  was increased logarithmically with time from  $(1.0 \rightarrow 1.8) \times 10^{-8}$  Torr. The Ga effusion cell temperature was kept constant at  $F_{Ga} = 1.0 \times 10^{-7}$  Torr. Si and Mg were used for n- and p-type doping, respectively. Devices A ( $\pi$ -doping, no QWs) and B ( $\pi$ -doping, 3 GaN QWs) were grown using these conditions. Figs. 2(a) and 2(b) show the measured and simulated x-ray diffraction (XRD) triple-axis  $\omega$ - $2\theta$  scans of the 2 samples obtained using PANalytical XRD system. X'pert epitaxy from PANalytical was used for simulation purposes.

The fringes around the primary GaN (002) peaks are due to the interference between layers of different compositions and thicknesses. The QWs in device B result in an increase in intensity and number of fringes. A linearly graded composition of AlGaIn was simulated with 100 steps. From the XRD scans the QW and barrier thicknesses were inferred to be  $t_w = 4.5$  nm and  $t_b = 19$  nm, respectively.

The samples were then processed into diodes by etching down to the n-type layer using Cl<sub>2</sub> based plasma in reactive ion etcher (RIE). The n-type contact metals (Ti/Au: 20 nm/200 nm) and p-type contact metals (Ni/Au: 20 nm/200 nm) were deposited by electron-beam evaporation. Thereafter, a wedge was cut from device B using focused ion beam (FIB) for transmission electron microscope (TEM) analysis. Fig. 2(c) shows a Z-contrast scanning transmission electron microscopy (STEM) micrograph of the processed GaN QW LED sample imaged at 300 keV electron energy. The Z-contrast is visible in the STEM image showing bright GaN QWs incorporated between the darker AlGaIn barriers. The graded layer goes from bright to dark as the AlGaIn composition increases. The layer thicknesses are consistent with those inferred from the XRD scan [Fig. 2(b)].

LED mesas of  $100 \times 125 \mu\text{m}^2$  size were tested for room temperature electrical and electroluminescence properties. The normalized room temperature EL spectrum of device B (with QWs) is shown in Fig. 3(a), showing a polarization-shifted emission peak at  $\lambda = 382$  nm corresponding to the QW optical transition energy. In addition, a shoulder (R) is observed extending to energies above the QW optical transition energy and beyond the GaN bandgap of 3.4 eV. This high energy emission shoulder is absent in the EL spectrum from device A [inset of Fig. 3(a)]. The emission at energies higher than QW optical transition energy signifies radiative recombination occurring in the graded AlGaIn layer due to partial electron spillover, indicated in the energy band diagram in Fig. 1(d) by "R". Fig. 3(b) shows the measured current/voltage characteristics of the diodes; a turn-on voltage near the band gap of GaN ( $\sim 3.4$  eV) and a high degree of rectification are observed. The lower current density for device B can be attributed to a higher contact resistance due to unoptimized p-type metal contact process for this sample, as can be inferred from the current/voltage characteristics. The results thus demonstrate the successful integration of quantum wells and polarization-induced p-type doping in N-polar III-nitride light emitting devices.

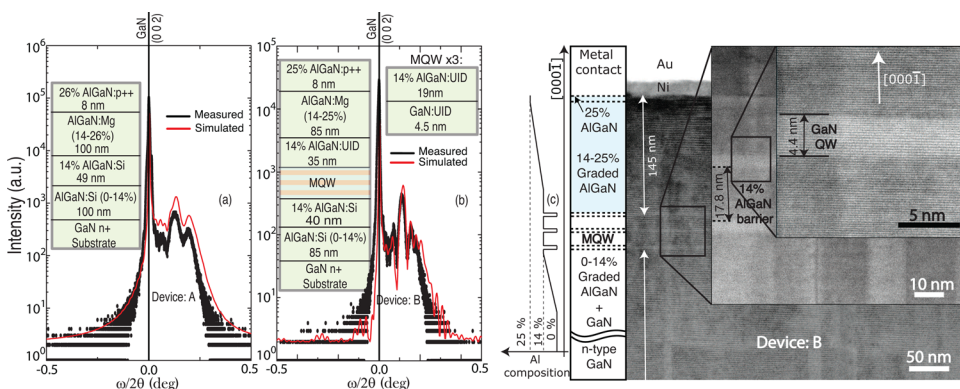


FIG. 2. (Color online) X-ray diffraction scans of (a) graded AlGaIn/GaN heterojunction [device A] and (b) QW UV-LED structure [device B]. The layer thicknesses and compositions indicated in the figure are obtained by comparing the simulated and measured data by careful fitting of the AlGaIn fringes and peaks on the right of the fundamental GaN (002) peak. (c) STEM scan of processed UV-LED structure [device B] showing three GaN QWs, the graded AlGaIn p-type layer, and the p-type contact metal. The variation of Al composition in various layers is sketched beside the LED structure.

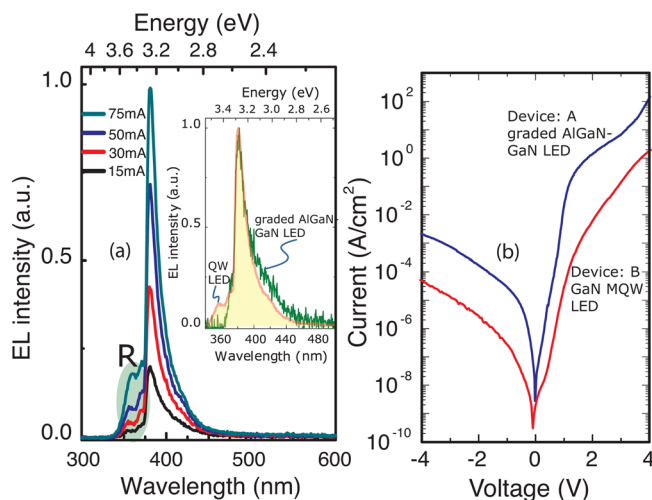


FIG. 3. (Color online) Electroluminescence spectrum of N-polar GaN UV LEDs. (a) The EL spectrum peaks at 382 nm with an emission shoulder [R: Fig. 1(d)] at energies larger than GaN bandgap. (a) Inset: EL spectrum of graded AlGaIn/GaN heterojunction (A) compared with GaN QW incorporated LED (B). The high energy shoulder is absent in emission from graded AlGaIn/GaN heterojunction; (b) current-voltage characteristics for devices A and B. Highly rectifying diodes with a turn-on voltage around 3.4 eV (the bandgap of GaN) are obtained.

In summary, a number of advantages of N-polar GaN heterostructures over metal-polar counterparts were outlined from the point of view of high-efficiency optical emitters such as LEDs and Lasers. N-polar heterostructures promise large improvements in the injection efficiency by (a) allowing for polarization-induced p-type doping and (b) aligning built-in electric fields such that they assist in the injection of electrons and holes into the quantum wells in the active region. N-polar GaN QW LEDs using polarization-induced p-type doping has been demonstrated in this work. The advantages and methods discussed can be exploited to improve the efficiencies of visible (blue/green) nitride LEDs and lasers. However, the ideas carry over to deep-UV light-

emitting devices based on heterostructures with very high Al composition AlGaIn layers, which are notoriously difficult to dope (both n- and p-type). It is in these devices that the properties of N-polar heterostructures potentially offer a window of opportunity to achieve higher efficiencies.

The authors acknowledge financial support from the DARPA CMUVT program (Dr. J. Albrecht).

- <sup>1</sup>S. Nakamura, M. Senoh, and T. Mukai, *Appl. Phys. Lett.* **62**, 2390 (1993).
- <sup>2</sup>T. Nishida and N. Kobayashi, *Phys. Stat. Sol. (a)* **176**, 45 (1999).
- <sup>3</sup>F. Bernardini and V. Fiorentini, *Phys. Stat. Sol. (a)* **190**, 65 (2002).
- <sup>4</sup>J. Piprek, *Nitride Semiconductor Devices Principles and Simulation* (Wiley-VCH Verlag, Weinheim, 2007), Chap. 3.
- <sup>5</sup>C. Wood and D. Jena, *Polarization Effects in Semiconductors: Ab Initio Theory to Device Applications* (Springer, Berlin, 2007), Chap. 2.
- <sup>6</sup>J. Simon, Z. Zhang, K. Goodman, H. Xing, T. Kosel, P. Fay, and D. Jena, *Phys. Rev. Lett.* **103**, 026801 (2009).
- <sup>7</sup>P. Waltereit, O. Brandt, A. Trampert, H. T. Grahn, J. Menniger, M. Ramsteiner, M. Reiche, and K. H. Ploog, *Nature* **406**, 865 (2000).
- <sup>8</sup>R. Dimitrov, M. Murphy, J. Smart, W. Schaff, J. R. Shealy, L. F. Eastman, O. Ambacher, and M. Stutzmann, *J. Appl. Phys.* **87**, 3375 (2000).
- <sup>9</sup>S. Rajan, M. Wong, Y. Fu, F. Wu, J. S. Speck, and U. K. Mishra, *Jpn. J. Appl. Phys.* **44**, L1478 (2005).
- <sup>10</sup>S. Krishnamoorthy, D. N. Nath, F. Akyol, P. S. Park, M. Esposto, and S. Rajan, *Appl. Phys. Lett.* **97**, 203502 (2010).
- <sup>11</sup>Z. Q. Li, M. Lestrade, Y. G. Xiao, and S. Li, *Phys. Stat. Sol. (a)* **208**, 928 (2011).
- <sup>12</sup>F. Akyol, D. N. Nath, E. Gur, P. S. Park, and S. Rajan, *Jpn. J. Appl. Phys.* **50**, 052101 (2011).
- <sup>13</sup>P. Kozodoy, H. Xing, S. P. DenBaars, U. K. Mishra, A. Saxler, R. Perrin, S. Elhamri, and W. C. Mitchel, *J. Appl. Phys.* **87**, 1832 (2000).
- <sup>14</sup>Y. Taniyasu, M. Kasu, and T. Makimoto, *Nature* **441**, 325 (2006).
- <sup>15</sup>Y. Liao, C. Thomidis, C. Kao, and T. D. Moustakas, *Appl. Phys. Lett.* **98**, 081110 (2011).
- <sup>16</sup>J. Simon, V. Protasenko, C. Lian, H. Xing, and D. Jena, *Science* **1**, 60 (2010).
- <sup>17</sup>C. H. Wang, C. C. Ke, C. Y. Lee, S. P. Chang, W. T. Chang, J. C. Li, Z. Y. Li, H. C. Kuo, T. C. Lu, and S. C. Wang, *Appl. Phys. Lett.* **97**, 261103 (2010).
- <sup>18</sup>K. Xu and A. Yoshikawa, *Appl. Phys. Lett.* **83**, 251 (2003).
- <sup>19</sup>T. Fujii, Y. Gao, R. Sharma, E. L. Hu, S. P. Denbaars, and S. Nakamura, *Appl. Phys. Lett.* **84**, 855 (2004).
- <sup>20</sup>Y. Gao, M. D. Craven, J. S. Speck, S. P. Denbaars, and E. L. Hu, *Appl. Phys. Lett.* **84**, 3322 (2004).